Friction **10**(2): 232–246 (2022)
https://doi.org/10.1007/s40544-020-0437-5
ISSN 2223-7690
CN 10-1237/TH
RESEARCH ARTICLE

Gelatin-based composite hydrogels with biomimetic lubrication and sustained drug release

Kuan ZHANG[1,2,†], Jielai YANG[3,4,†], Yulong SUN[1], Yi WANG[1], Jing LIANG[4], Jing LUO[5], Wenguo CUI[4], Lianfu DENG[4], Xiangyang XU[3,*], Bo WANG[2,*], Hongyu ZHANG[1,*]

[1] *State Key Laboratory of Tribology, Department of Mechanical Engineering, Tsinghua University, Beijing 100084, China*

[2] *School of Chemical and Biological Engineering, Shandong University of Science and Technology, Qingdao 266590, China*

[3] *Department of Orthopedics, Ruijin Hospital, Shanghai Jiao Tong University School of Medicine, Shanghai 200025, China*

[4] *Shanghai Key Laboratory for Prevention and Treatment of Bone and Joint Diseases, Shanghai Institute of Traumatology and Orthopaedics, Ruijin Hospital, Shanghai Jiao Tong University School of Medicine, Shanghai 200025, China*

[5] *Beijing Research Institute of Automation for Machinery Industry Co., Ltd., Beijing 100120, China*

Received: 12 June 2020 / Revised: 27 July 2020 / Accepted: 30 July 2020

Abstract: The occurrence of osteoarthritis is closely related to progressive and irreversible destruction of the articular cartilage, which increases the friction significantly and causes further inflammation of the joint. Thus, a scaffold for articular cartilage defects should be developed via lubrication restoration and drug intervention. In this study, we successfully synthesized gelatin-based composite hydrogels, namely GelMA–PAM–PMPC, with the properties of biomimetic lubrication and sustained drug release by photopolymerization of methacrylic anhydride modified gelatin (GelMA), acrylamide (AM), and 2-methacryloyloxyethyl phosphorylcholine (MPC). Tribological test showed that the composite hydrogels remarkably enhanced lubrication due to the hydration lubrication mechanism, where a tenacious hydration shell was formed around the zwitterionic phosphocholine headgroups. In addition, drug release test indicated that the composite hydrogels efficiently encapsulated an anti-inflammatory drug (diclofenac sodium) and achieved sustained release. Furthermore, the *in vitro* test revealed that the composite hydrogels were biocompatible, and the mRNA expression of both anabolic and catabolic genes of the articular cartilage was suitably regulated. This indicated that the composite hydrogels could effectively protect chondrocytes from inflammatory cytokine-induced degeneration. In summary, the composite hydrogels that provide biomimetic hydration lubrication and sustained local drug release represent a promising scaffold for cartilage defects in the treatment of osteoarthritis.

Keywords: hydrogel; articular cartilage; zwitterionic polymer; hydration lubrication; drug delivery

1 Introduction

From a biotribological viewpoint, osteoarthritis has been accepted as a lubrication deficiency-induced joint disease that is characterized by the breakdown of articular cartilage and inflammation of the joint. Therefore, a synergetic therapy integrating both lubrication and drug intervention is a promising approach for the treatment of osteoarthritis [1, 2]. However, due to the insufficiency of blood vessels in articular cartilage, it is very difficult for nutritious agents/drugs to reach the joint via oral administration [3, 4]. Thus, the design of a scaffold to simultaneously achieve enhanced lubrication and sustained drug

† Kuan ZHANG and Jielai YANG contributed equally to this work.
* Corresponding authors: Xiangyang XU, E-mail: xu664531@163.com; Bo WANG, E-mail: wb@sdust.edu.cn; Hongyu ZHANG, E-mail: zhanghyu@tsinghua.edu.cn

delivery is a good solution for cartilage defects, although this subject is still facing great challenges.

Hydrogels have been widely studied as an ideal substitute for articular cartilage and as a drug carrier. Great effort has been devoted to designing functional hydrogels with good biocompatibility [5], high mechanical strength [6], and low coefficient of friction (COF) [7, 8]. Recently, many hydrogels have been developed to exhibit excellent physicochemical properties such as double-network hydrogels [9], mussel-inspired functional hydrogels [10–12], composite hydrogels [13], and hydrogen-bonded crosslinked hydrogels [14]. Gelatin, a single-chain derivative formed by collagen, is biocompatible and can be biodegraded *in vivo*. Additionally, the side chains of gelatin are rich in reactive groups (–COOH and $–NH_2$), and thus different gelatin hydrogels (GelMA) have been synthesized to repair skin, bone, and articular cartilage [15, 16], in which methacrylic anhydride is introduced to initiate photopolymerization [17, 18]. However, to the best of our knowledge, the lubrication properties of GelMA hydrogels have rarely been investigated.

Many methods have been reported for improving the mechanical properties of hydrogels, but the improvement in mechanical properties often compromises lubrication [19–21]. Naturally, articular cartilage has an ultra-low COF (at a level of 0.001–0.01) based on hydration lubrication mechanism [22–24], where polyelectrolyte biomacromolecules (such as hyaluronic acid, aggrecan, and lubricin) complex with phosphatidylcholine (PC) lipids form a lubricating boundary layer by exposing the hydrated phosphocholine groups ($N^+(CH_3)_3$ and PO_4^-) on the superficial surface [25]. Poly(2-methacryloyloxyethyl phosphorylcholine) (PMPC), a biocompatible polymer, has the same zwitterionic phosphocholine groups as PC lipids, and it has been widely used to enhance the lubrication properties of various biomedical materials through surface modification [26–28].

In this study, bioinspired by the hydration lubrication mechanism of articular cartilage, we developed gelatin-based composite hydrogels with biomimetic lubrication and sustained drug release (GelMA–PAM–PMPC). Specifically, acrylamide (AM) and MPC were introduced into GelMA to improve the mechanical and lubrication properties of the composite hydrogels. Additionally, diclofenac sodium (DS, a typical anti-inflammatory drug to relieve pain due to osteoarthritis) was encapsulated while preparing the composite hydrogels. It is hypothesized that the dual-functional composite hydrogels developed herein, as a scaffold for cartilage defects to achieve both lubrication enhancement and local drug delivery, may find applications in the treatment of osteoarthritis.

2 Materials and methods

2.1 Materials and reagents

2-Methacryloyloxyethyl phosphorylcholine (MPC) was obtained from Joy-Nature Co. (Nanjing, China). Gelatin was purchased from Sinopharm Chemical Reagent Co., Ltd. (Shanghai, China). Methacrylic anhydride and DS were purchased from J&K Scientific Ltd. (Beijing, China). Ethyl acetate was purchased from Modern Oriental Technology Development Co., Ltd. (Beijing, China). Dulbecco's modified eagle's medium (DMEM)/nutrient mixture F-12 medium, bovine serum albumin, fetal bovine serum, and 0.25% trypsin-ethylenediaminetetraacetic acid (trypsin-EDTA) were purchased from Gibco Life Technologies Corp. (CA, USA). Live/dead viability/cytotoxicity kit was purchased from Invitrogen (Carlsbad, CA, USA). Cell counting kit-8 (CCK-8) was purchased from Dojindo Molecular Technologies, Inc. (Kumamoto, Japan). SYBR® Green PCR Master Mix (DRR420A) and Prime Script RT reagent kit (DRR037A) were provided by Takara Biomedical Technology (Beijing) Co., Ltd. (Tokyo, Japan). Phalloidin was purchased from Sigma-Aldrich Co. (St. Louis, MO, USA). Recombinant mouse IL-1β and TNF-α were purchased from PeproTech (Rocky Hill, NJ, USA).

2.2 Synthesis of composite hydrogels

GelMA was synthesized according to previously described methods [29, 30]. Gelatin (5 g) was added to phosphate buffer solution (PBS, 50 mL) and magnetically stirred at 50 °C until it was completely dissolved. Then, methacrylic anhydride (5 mL) was added dropwise to the above solution (0.5 mL/min) and reacted in a 50 °C isothermal water bath under magnetic stirring. After 4 h, the reaction solution was diluted with PBS (200 mL, 50 °C) and stirred to terminate the reaction. The above solution was placed

in a dialysis bag (molecular weight cutoff: 8–14 kDa) and dialyzed in pure water at 50 °C for 6 d. The dialyzed solution was poured into a centrifuge tube for centrifugation (2,500 rpm), and the supernatant was transferred and lyophilized to obtain the GelMA product.

The synthesis of the composite hydrogels was achieved by photopolymerization. Briefly, GelMA (1 g), MPC (mass ratio to GelMA: 5%, 15%, 30%, and 50%), crosslinker (bis-acrylamide, 1%), and photoinitiator (I2959-Tos, 5 mg) were added to the AM solution to pre-polymerize the monomers at 37 °C. Subsequently, the pre-polymerized solution was transferred to a custom-made mold and irradiated using an ultraviolet spot light source (7.1 mW/cm^2, 360–480 nm) for 5 min. Finally, the hydrogels (GelMA–PAM–PMPC) were taken out and soaked in PBS at 37 °C for 24 h to remove the uncrosslinked monomers. Pure GelMA–PAM and GelMA hydrogels were prepared using the same method. Unless mentioned otherwise, the GelMA–PAM–PMPC samples used in the following tests contained 30% MPC.

2.3 Characterization of composite hydrogels

^{1}H nuclear magnetic resonance (NMR) spectra of gelatin and GelMA were recorded using an Ascend 400 MHz NMR spectrometer (Bruker, USA) with D_2O as the solvent. Fourier transform infrared (FTIR) spectra of PMPC, GelMA, and GelMA–PAM–PMPC were analyzed using a Nexus 670 spectrometer (Nicolet, USA) at 400–4,000 cm^{-1}. The water content of GelMA and GelMA–PAM–PMPC was measured via thermogravimetric analysis (TGA) (Q5000IR, TA Instruments, USA) from 25 to 300 °C at a heating rate of 10 °C /min.

To examine the swelling behavior of the hydrogels, GelMA and GelMA–PAM–PMPC were incubated in PBS at 37 °C and sampled at 0, 0.5, 1, 3, and 5 h after incubation. Then, the hydrogels were freeze-dried, and the swelling ratio (λ_w) and the relative volume (λ_v) were calculated using Eqs. (1) and (2).

$$\lambda_w = \frac{W_i}{W_0} \tag{1}$$

$$\lambda_v = \frac{\pi \times R_i^2 \times H_i}{\pi \times R_0^2 \times H_0} \tag{2}$$

Here, W_i and W_0 are the swollen and dry weights of the hydrogels, respectively, which were measured in an equilibrium state. The swelling ratio (λ_w) was calculated as the ratio of the weight of swollen hydrogels to that of dry hydrogels (Eq. (1)). R_i, R_0, H_i, and H_0 are the radius and height of the hydrogels (cylindrical samples) before and after swelling, respectively. The relative volume (λ_v) was calculated as the ratio of the volume of swollen hydrogels to that of dry hydrogels (Eq. (2)).

The water contact angle of GelMA and GelMA–PAM–PMPC was obtained using an OCA25 contact angle goniometer (Dataphysics Instruments, Germany) by the sessile drop method. Distilled water (3 μL) was placed on the airside surface of the hydrogels at room temperature, and the static contact angle was collected after 10 s. The mean contact angle was calculated from the results of at least three measurements.

To depict the internal microstructures of the hydrogels, GelMA and GelMA–PAM–PMPC were freeze-dried to thoroughly remove water. Subsequently, the hydrogels were coated with Pt/Pd and examined using a Quanta 200 field emission scanning electron microscope (SEM, FEI, Eindhoven, Netherlands) under an accelerating voltage of 5 kV, which was coupled with energy dispersive spectroscopy (EDS) to enable elemental composition analysis. Image J software was used to quantify the pore distribution of the hydrogels based on a series of SEM images. The pores were randomly selected on the surface of the hydrogels. The pore size was nominated as the average pore diameter on the selected SEM images.

The mechanical properties of GelMA and GelMA–PAM–PMPC were evaluated using a Zwick Z020 universal testing machine (ZwickRoell, Germany) with a 0.25 kN load cell. The hydrogels used for the compressive performance test were cut into cylindrical shapes (diameter: 15 mm; length: 15 mm). During the compressive tests, the speed of the crosshead was maintained at 0.5 mm/min until the hydrogels failed. A series of five samples were evaluated to ensure the reproducibility of the data.

2.4 *In vitro* drug loading and release

Initially, a calibration curve of the drug DS in PBS at various concentrations (5, 10, 15, 20, and 25 μg/mL) was obtained by measuring the absorbance value using a UV-vis spectrophotometer (UV-8000s, Metash

Instruments, China) at 276 nm, as displayed in Fig. S1 in the Electronic Supplementary Material (ESM). To load the drug, GelMA and GelMA–PAM–PMPC (100 mg) were added to the DS solution in PBS (20 mL) and uniformly dispersed by ultrasound. The mixture was stirred for 12 h, and the hydrogels were removed and washed with deionized water several times. The DS remaining in PBS was monitored according to the calibration curve. Similarly, the DS released from the hydrogels at various intervals was evaluated using a UV-vis spectrophotometer. The test for drug release was performed until the solution concentration remained nearly constant. The drug loading capacity (LC), encapsulation efficiency (EE), and cumulative drug release of the hydrogels were calculated using Eqs. (3)–(5). Each test was repeated three times from which the mean value was calculated.

$$\mathrm{LC}(\%) = \frac{\text{amount of loaded DS}}{\text{amount of DS-loaded hydrogels}} \cdot 100 \quad (3)$$

$$\mathrm{EE}(\%) = \frac{\text{amount of loaded DS}}{\text{amount of added DS}} \cdot 100 \quad (4)$$

$$\text{Drug release}(\%) = \frac{M_t}{M_a} \cdot 100 \quad (5)$$

Here, M_t is the amount of DS released from the hydrogels at time t, while M_a is the DS encapsulated in the hydrogels.

2.5 Lubrication properties

The lubrication properties of the hydrogels were evaluated by a tribological test, which was performed on a UMT-3 universal material tester (Center for Tribology Inc., USA) operated in a pin-on-disk rotating mode (rotation radius: 2 mm). The hydrogels (GelMA–PAM and GelMA–PAM–PMPC) were fixed to the platform of the tester with cyanoacrylate glue. The contact pair was a sphere (bearing steel GCr15) with a radius of 3 mm. Tribological tests were conducted at 25 °C under various experimental conditions: the content of MPC (0%, 5%, 15%, 30%, and 50%), normal load (0.1, 0.2, 0.5, 1, and 2 N), and rotation frequency (0.5, 1, 2, and 5 Hz). Tribological tests were performed for 10 min, and sufficient deionized water was added to the surface of the hydrogels as a lubricant. The tribological test under each condition was performed at least three times to obtain reliable data, and the mean COF was then recorded. After the tribological test, the surface topology of the hydrogels and the steel spheres was evaluated using an optical interferometer (NeXView, ZYGO, USA), and the surface roughness values (Sa) of the samples were obtained from at least three measurements at random positions on the surface [31].

2.6 Primary chondrocytes isolation and culture

Articular cartilage was collected from mice (C57B/L6, male, 4-7 days old, Ruijin Hospital, School of Medicine, Shanghai Jiao Tong University). The pieces of articular cartilage were dissected and separated aseptically from the underlying bone and connective tissues. The cartilage was then cut into small pieces, washed with PBS, and digested using collagenase type II (0.2%) at 37 °C for 4 h. Afterward, the cartilage tissues were suspended and seeded into tissue culture plates in an incubator (37 °C and 5% CO_2). The culture medium was Dulbecco's modified eagle medium (DMEM)/nutrient mixture F-12, which was supplemented with 1% penicillin/streptomycin antibiotics and 10% fetal bovine serum. The cells were passaged using 0.25% trypsin-EDTA solution when the confluence reached approximately 80%–90%. Leach solution of hydrogel materials was used for all the following cell experiments.

2.7 Cell proliferation

Cell cytotoxicity was evaluated using a CCK-8 kit with reference to the manufacturer's instructions. Briefly, primary chondrocytes were cultured in 96-well plates at 1×10^4 cells per well. The culture plates were placed in a humidified atmosphere of 37 °C and 5% CO_2 during incubation. After co-culturing with GelMA and GelMA–PAM–PMPC hydrogels for 1, 3, and 5 days, the cells were washed with PBS, and 10 μL of the CCK-8 solution was added to each well, before being further cultured at 37 °C for another 2 h. Subsequently, the solution absorbance was measured at 450 nm using a multiskan spectrum microplate photometer (Thermo Scientific, Finland). The group treated with untreated chondrocytes was assigned to the blank group. Three replicates of each group were evaluated and shown as optical density, which directly correlated to the number of viable cells.

2.8 Cell morphology and viability

The chondrocytes were seeded on glass coverslips and then co-cultured with the GelMA and GelMA–PAM–PMPC hydrogels for 1, 3, and 5 days. The effect of GelMA and GelMA–PAM–PMPC hydrogels on the morphology and viability of chondrocytes was evaluated using a live/dead cell kit (Life Tech, USA). After co-culturing with the hydrogels for 1, 3, and 5 days, ethidium homodimer-1 (2 μL) and calcein acetomethoxy (0.5 μL) were mixed with DMEM (1 mL) for staining the cells in the dark for 30 min. Following incubation, the constructs were washed with PBS three times and observed using a fluorescent microscope (Axio Imager M1, ZEISS, Germany). The group treated with untreated chondrocytes was assigned to the blank group.

2.9 Phalloidin staining

The chondrocytes were plated on glass coverslips and then co-cultured with the GelMA and GelMA–PAM–PMPC hydrogels for 1, 3, and 5 days following the procedure described above. The attached cells were fixed using paraformaldehyde (4%) and permeabilized with Triton X-100 (0.2%) for 10 min. Afterward, the cells were stained with 100 nM Alexa Fluor 488-conjugated phalloidin (A12379, Thermo Fisher) for 30 min in the dark and then fixed with paraformaldehyde (4%) for 20 min. After washing with PBS, the stained cells were observed using a laser scanning confocal microscope (LSM800, ZEISS, Germany). The group treated with untreated chondrocytes was assigned to the blank group.

2.10 Real-time quantitative polymerase chain reaction (RT-qPCR) assay

To investigate the protection of the hydrogels for inflammation-induced chondrocyte degeneration, the RT-qPCR assay was used to analyze the expression levels of cartilage-specific genes such as COL2A1, aggrecan, ADAMTS5, and MMP13. The chondrocytes were seeded in 6-well plates at 1×10^5 cells per well, stimulated with TNF-α or IL-1β (concentration: TNF-α (5 ng/mL) or IL-1β (10 ng/mL)), and treated with GelMA and GelMA–PAM–PMPC hydrogels simultaneously for 24 h. The total RNA of chondrocytes was extracted from the cells using TRIzol reagent (Invitrogen, USA). RNA (1 μg) was reverse transcribed to synthesize complementary DNA (cDNA). For RT-qPCR, 10 μL of reaction volume was applied, that is, 5 μL of 2X SYBR Master Mix, 4.5 μL of diluted cDNA, and 0.25 μL of each primer. The parameters of RT-PCR were set as follows: 95 °C for 10 min, followed by 40 cycles at 95 °C for 15 s and 60 °C for 1 min. The procedure was conducted using an ABI 7500 Sequencing Detection System (Applied Biosystems, CA, USA). The values of cycle threshold (Ct) were obtained and normalized to β-actin. The relative mRNA level of each gene was evaluated based on the $2^{-\Delta\Delta Ct}$ method [33]. The primers were designed with the aid of the NCBI Primer-Blast Tool, as shown in Table 1. The group using chondrocytes treated with TNF-α or IL-1β was assigned to the blank group.

2.11 Statistical analysis

Quantitative data are presented as mean ± standard deviation. Independent tests were repeated at least three times to verify the results. One-way analysis of variance was performed to detect significant differences between separate groups. Statistical analysis was conducted using GraphPad Prism software (GraphPad Software Inc., USA). The level of significance was displayed as $^*P < 0.05$, $^{**}P < 0.01$.

Table 1 The primer sequences of the genes used in the study.

Genes	Forward sequence	Reverse sequence
Aggrecan	5’-TGCAGGACCAGACCGTCAGATAC-3’	5’-CGAGGCGTGTGGCGAAGAAC-3’
COL2A1	5’-TACTGGAGTGACTGGTCCTAAG-3’	5’-AACACCTTTGGGACCATCTTTT-3’
MMP13	5’-AACACCTTTGGGACCATCTTTT-3’	5’-GTCACACTTCTCTGGTGTTTTG-3’
ADAMTS5	5’-GGCAAATGTGTGGACAAAACTA-3’	5’-GAGGTGCAGGGTTATTACAATG-3’
β-actin	5’-CTACCTCATGAAGATCCTGACC-3’	5’-CACAGCTTCTCTTTGATGTCAC-3’

3 Results and discussion

3.1 Design of composite hydrogels

We successfully developed gelatin-based composite hydrogels with the properties of biomimetic lubrication and sustained local drug release (GelMA–PAM–PMPC) that could function as a cartilage substitutional scaffold for treating osteoarthritis. As shown in Fig. 1(a), the composite hydrogels were synthesized via photopolymerization of GelMA, AM, and MPC, using I2959-Tos as the initiator, which was developed in our previous study [34]. The crosslinked network of the composite hydrogels included physical (e.g., entangled chains and hydrogen bonding in gelatin) and chemical (e.g., covalent bonds between the monomers) crosslinking, which enhanced the mechanical properties of the composite hydrogels. As shown in Fig. 1(b), the lubrication property of the composite hydrogels was assessed by a series of tribological tests, which were performed on a ball-on-disk rotating tribometer. The zwitterionic phosphocholine groups ($N^+(CH_3)_3$ and PO_4^-) in PMPC, bioinspired by the hydration lubrication mechanism of articular cartilage, contributed to the lubrication enhancement. Additionally, the composite hydrogels were encapsulated with the drug DS during preparation to endow the hydrogels with sustained drug release behavior. The chondroprotective potential of the composite hydrogels was verified by analyzing the mRNA expression levels of cartilage-specific genes following co-culturing with the cytokine-treated chondrocytes.

3.2 Characterization of composite hydrogels

The ^{1}H NMR spectra of gelatin and GelMA are displayed in Figs. 2(a) and 2(b). The distinct double peak at 5.36 and 5.64 ppm corresponds to the CH_2=C(CH_3)– proton peak. This indicates that the methacrylic group is successfully grafted onto the molecular chain of gelatin. The FTIR spectra of PMPC, GelMA, and GelMA–PAM–PMPC are presented in Fig. 2(c). The absorption peaks at 1,350 and 1,450 cm^{-1} are observed for GelMA–PAM–PMPC and are attributed to the amide groups in PAM. Additionally, compared with GelMA, new absorption peaks appear at 950, 1,230, and 1,720 cm^{-1} for GelMA–PAM–PMPC, corresponding to the P–O, P=O, and C=O groups in PMPC, respectively. This indicates that the composite hydrogels GelMA–PAM–PMPC have been successfully synthesized by photopolymerization.

The TGA curves of GelMA and GelMA–PAM–PMPC

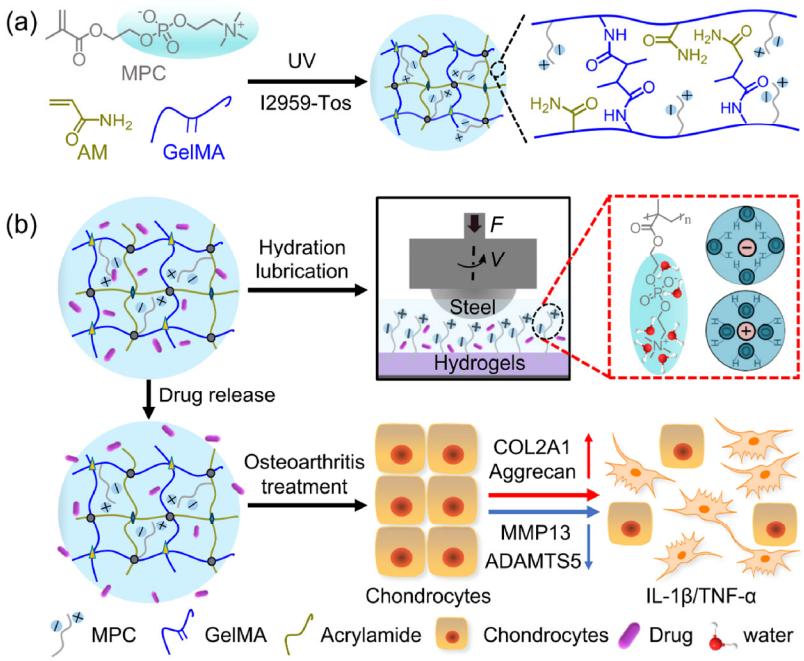

Fig. 1 Schematic illustration of gelatin-based composite hydrogels for the treatment of osteoarthritis with biomimetic lubrication and sustained drug release. (a) Synthesis of the composite hydrogels through photopolymerization. (b) Lubrication enhancement and chondroprotective potential of the hydrogels.

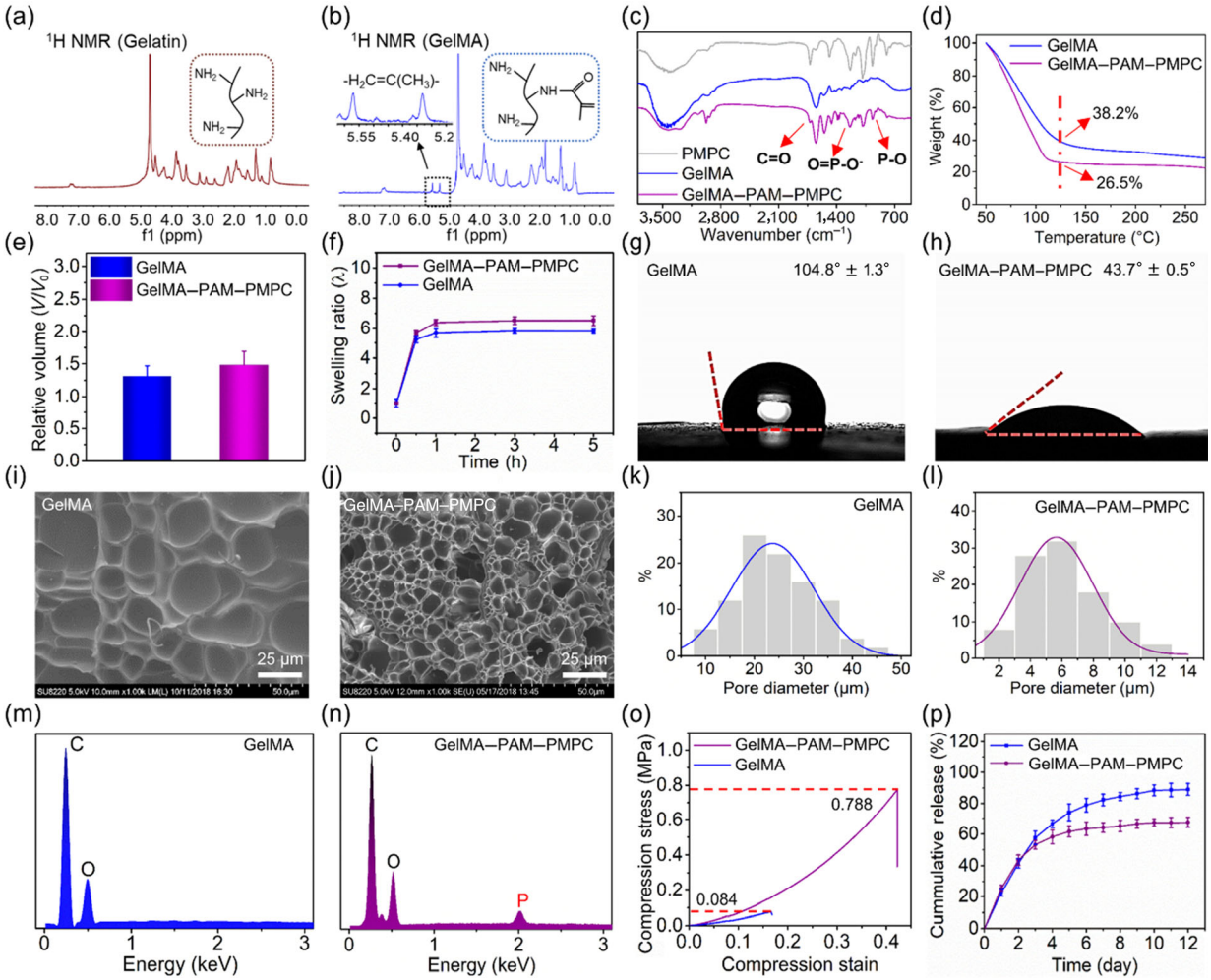

Fig. 2 Characterization of the composite hydrogels. ^{1}H NMR spectrum of (a) gelatin and (b) GelMA. (c) FTIR spectrum of PMPC, GelMA, and GelMA–PAM–PMPC. (d) TGA curve, (e) relative volume, (f) swelling ratio of GelMA and GelMA–PAM–PMPC. Water contact angle, SEM image, pore distribution, EDS spectrum of (g, i, k, m) GelMA and (h, j, l, n) GelMA–PAM–PMPC. (o) Compression stress, and (p) drug release profile of GelMA and GelMA–PAM–PMPC.

are shown in Fig. 2(d). The water content of GelMA and GelMA–PAM–PMPC is 61.8% and 73.5%, respectively. The higher water content of GelMA–PAM–PMPC, compared with GelMA, is attributed to the introduction of PMPC, which is regarded as a superhydrophilic material in the presence of phosphocholine groups [35]. The relative volume, swelling ratio, and water contact angle of GelMA and GelMA–PAM–PMPC are illustrated in Figs. 2(e)–2(h). For the same reason, the swelling ratio and relative volume of GelMA–PAM–PMPC are higher than those of GelMA, and the water contact angle of GelMA–PAM–PMPC (43.7° ± 0.5°) is much lower than that of GelMA (104.8° ± 1.3°). With the incubation of the hydrogels in PBS, the swelling ratio of GelMA and GelMA–PAM–PMPC increases greatly during the initial 1 h and reaches equilibrium after 3 h. However, the relative volume of GelMA and GelMA–PAM–PMPC remains unaffected after incubation, which is beneficial when the hydrogels are applied as a scaffold for cartilage defects.

The cross-sectional microstructure, pore size distribution, and elemental composition of GelMA and GelMA–PAM–PMPC examined by SEM and EDS are shown in Figs. 2(i)–2(n). GelMA has a highly interconnected and loose porous network with a pore size of approximately 30 μm. Compared with GelMA, the microstructure of GelMA–PAM–PMPC is denser, and the pore size reduces dramatically (to ~6 μm), which is attributed to the increase in the covalent crosslinking of the hydrogels. Additionally, the

detection of P for GelMA–PAM–PMPC further confirms that the development of composite hydrogels has been successful.

Mechanical strength is one of the key factors for cartilage substitutional scaffolds, especially when the hydrogels should provide sufficient mechanical support during the early stage of implantation before adapting to surrounding cartilage tissues. The compressive strength of GelMA and GelMA–PAM–PMPC is shown in Fig. 2(o). Compressive strength of GelMA–PAM–PMPC (0.788 MPa at 42% compression strain) is significantly improved than that of GelMA (0.084 MPa at 14% compression strain). This result is attributed to the chemically covalent crosslinking and the corresponding increase in the density of the microstructure of the hydrogels. Generally, gelatin forms physically crosslinked hydrogels by its own hydrogen bonding, and the introduction of methacrylic anhydride, AM, and MPC generates chemically crosslinked hydrogels by UV-induced photopolymerization.

3.3 *In vitro* drug loading and release

The *in vitro* drug loading and release of the hydrogels was investigated using DS as a nonsteroidal anti-inflammatory drug for the treatment of osteoarthritis at 37 °C. The LC and EE of GelMA–PAM–PMPC (10.9%, 49.2%) are slightly higher than that of GelMA (9.5%, 42.1%). The drug release profile of DS-loaded GelMA and GelMA–PAM–PMPC is shown in Fig. 2(p). Both curves display an initial rapid drug release, which is followed by a plateau stage. After 10 days, 88.7% of DS is released from GelMA, which is much higher than that of GelMA–PAM–PMPC (64.5%). DS released from GelMA–PAM–PMPC is lower at each time interval, compared with GelMA, which indicates that the composite hydrogels can achieve a sustained drug release of DS.

3.4 Lubrication property of composite hydrogels

A series of tribological tests were performed to reveal the lubrication properties of the composite hydrogels, as shown in Fig. 3(a). Before the tribological tests, the surface roughness of GelMA–PAM and GelMA–PAM–PMPC is measured to be 218 and 284 nm, respectively (Figs. 3(b) and 3(c)). The COF of GelMA–PAM–PMPC with various MPC contents is displayed in Fig. 3(d) (load: 0.5 N; frequency: 2 Hz). The lubrication of the composite hydrogels is highly dependent on the MPC content, and with the increase in the MPC content, the COF value decreases significantly from 0.052 (0%) to 0.011 (30%). A further increase in the MPC content to 50% does not improve the lubrication. Consequently, this setup is applied in the tribological tests under different conditions.

Hydrogels are viscoelastic and the surface physicochemical properties can result in a complex lubrication performance [36, 37]. The lubrication of hydrogels is related to the applied load and rotation frequency, which is investigated and illustrated in Figs. 3(e) and 3(f). The COF values of GelMA–PAM and GelMA–PAM–PMPC increase greatly from 0.042 to 0.063 and from 0.014 to 0.041 when the normal load changes from 0.1 to 2 N. This result is attributed to the effect of the normal load on the contact stress and deformation of the hydrogels, as schematically shown in Fig. 3(g). Under a higher normal load, with the increase in the contact stress and indentation depth, the lateral friction force will be greatly increased, thus resulting in a larger COF value. Additionally, the COF value of GelMA–PAM–PMPC slightly decreases from 0.018 to 0.011 when the rotation frequency increases from 0.5 to 5 Hz, and a similar trend is obtained for GelMA. The short contact time of slip at a high rotation frequency produces an effective hydration interface between the tribopairs, which can result in a reduced COF value [38, 39]. Under each experimental condition, the COF value of GelMA–PAM–PMPC is lower than that of GelMA–PAM, although it has a relatively high surface roughness. This indicates that the enhanced lubrication of the composite hydrogels is due to the introduction of the PMPC.

The zwitterionic phosphocholine groups ($N^+(CH_3)_3$ and PO_4^-) in PMPC are the same as that in the PC lipids, which form a complex with the polyelectrolyte biomacromolecules and dominate the superlubrication of articular cartilage based on hydration lubrication. Phosphocholine groups can attract water molecules to form a tenacious hydration shell around the charges as a result of the interaction between the water dipole and enclosed zwitterionic charges [40]. The hydration shell not only supports high pressures

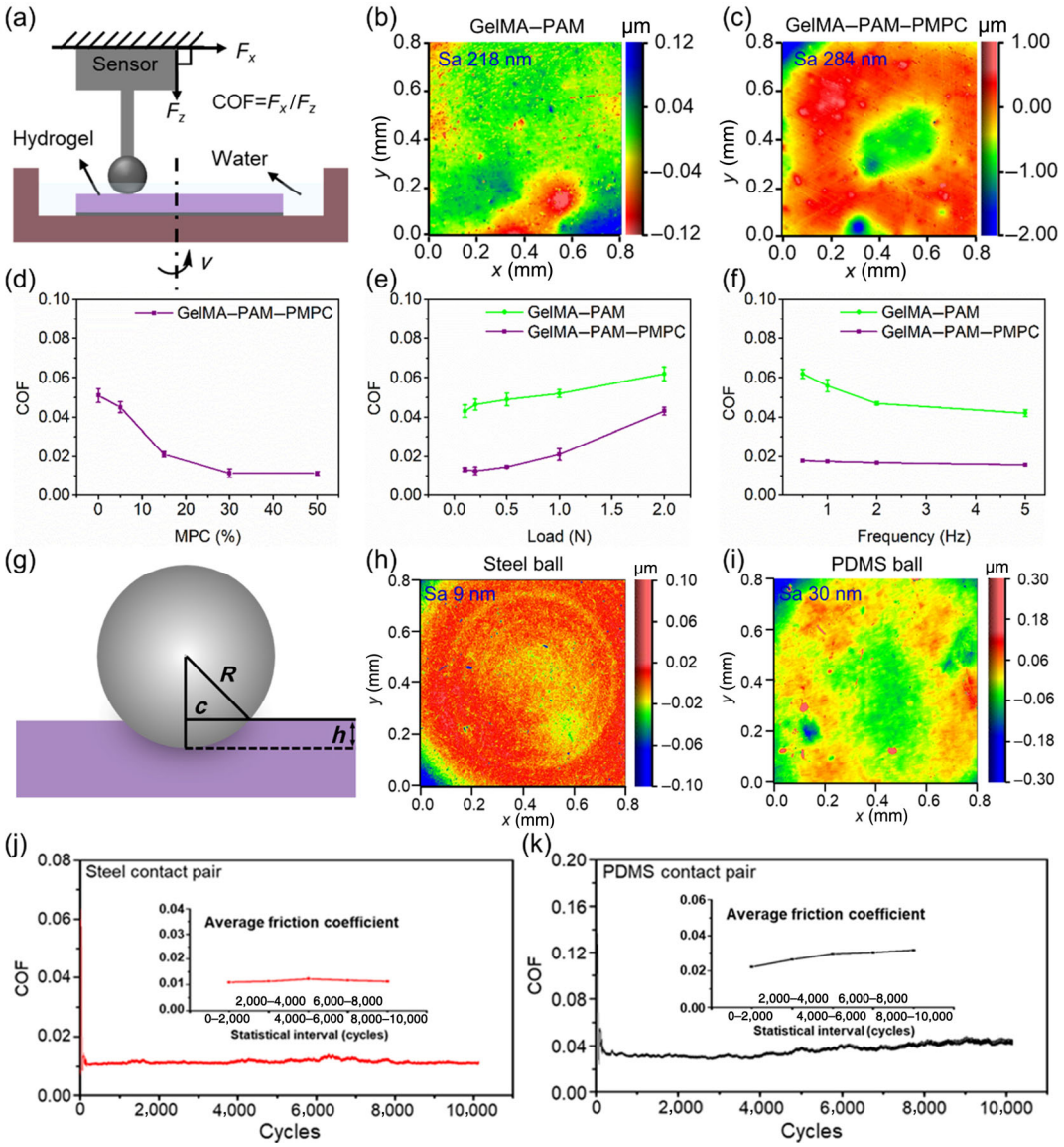

Fig. 3 Lubrication property of composite hydrogels. (a) Schematic diagram showing the setup of the tribological test. Surface topography contour of (b) GelMA–PAM and (c) GelMA–PAM–PMPC. (d) COF of GelMA–PAM–PMPC with different MPC contents. COF of GelMA–PAM and GelMA–PAM–PMPC with (e) various normal loads, rotation frequency: 5 Hz and (f) various rotation frequencies, normal load: 0.5 N. (g) Schematic diagram showing the deformation of the hydrogels under applied normal load. Surface topography contour of (h) steel ball and (i) PDMS ball. COF-cycle curve for (j) steel contact pair and (k) PDMS contact pair. Inset figure shows the average COF calculated from different cycle intervals.

without being squeezed out but also behaves in a fluidlike manner under shear, leading to a significant reduction in the interfacial friction under various test conditions [41]. Therefore, the composite hydrogels GelMA–PAM–PMPC can enhance lubrication owing to the hydration lubrication mechanism. Additionally, the excellent water trapping capability of the composite hydrogels due to interconnected porous microstructure also contributes to maintaining good lubrication performance.

The optimal scaffold for repairing articular cartilage defects should maintain a low COF value after multiple testing cycles [42]. To examine the durability of the composite hydrogels, hard steel and soft polydimethylsiloxane (PDMS) balls were employed as tribopairs to slide against the hydrogels under a normal load of 0.5 N and a rotation frequency of 5 Hz, with an extended duration of 10,000 cycles.

The surface roughness of the steel ball and PDMS ball is approximately 9 and 30 nm, respectively, as shown in Figs. 3(h) and 3(i). It is indicated from Figs. 3(j) and 3(k) that the COF value remains relatively unchanged during the test. A lower COF value is obtained using steel ball as the contact tribopair, compared with the PDMS ball, although the contact stress between the steel ball and the hydrogels is much larger than that between the PDMS ball and the hydrogels (as the elastic modulus of steel is much higher than that of PDMS). The larger COF value using the PDMS ball as the contact tribopair is attributed to its higher surface roughness. The above results indicate that the composite hydrogels can sustain low friction under extended loading cycles, especially when sliding against a steel ball.

3.5 Cell cytotoxicity and protection for chondrocytes degeneration

To evaluate the potential clinical application of the composite hydrogels, we investigated the *in vitro* cytotoxicity of GelMA and GelMA–PAM–PMPC on primary mouse chondrocytes and performed tests to determine whether GelMA and GelMA–PAM–PMPC can protect against chondrocyte degeneration. The hydrogel samples used in the following tests were encapsulated with DS.

The live/dead assay and CCK-8 test were conducted to examine the cytotoxicity of the hydrogels on cell viability and proliferation of primary mouse chondrocytes. Figures 4(a)–4(c) show the results of the live/dead assay after co-culturing the chondrocytes with GelMA and GelMA–PAM–PMPC for 1, 3, and 5 days, where the dead cells are labeled red and living cells green. Most of the seeded chondrocytes are alive during culturing, and the density of the cells increases from day 1 to day 5. The viability of the chondrocytes co-cultured with the hydrogels is almost the same as that of the blank group for all incubation times, indicating that the hydrogels are highly biocompatible with no detrimental effect on the chondrocytes. Overall, there are no significant differences in the live/dead cells among the blank, GelMA, and GelMA–PAM–PMPC groups at different time intervals.

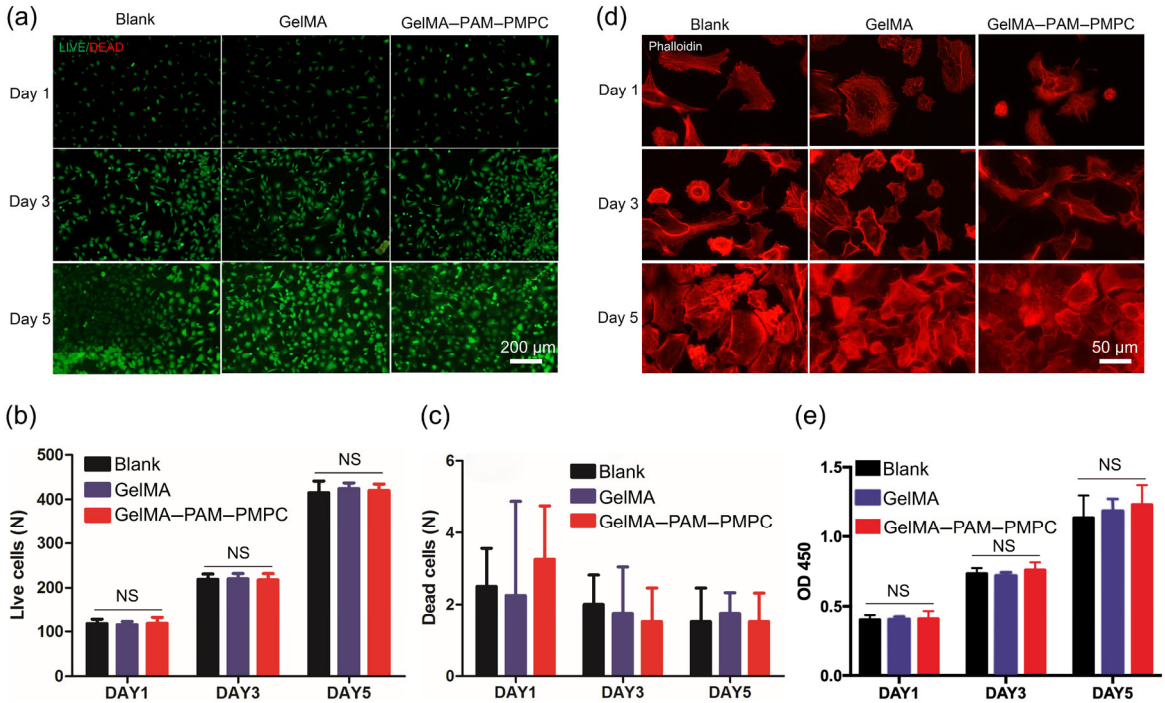

Fig. 4 *In vitro* cell viability and proliferation of the chondrocytes incubated with the GelMA and GelMA–PAM–PMPC hydrogels for 1, 3, and 5 days. Blank group: untreated chondrocytes. (a) Representative fluorescence images of the chondrocytes in live/dead cell staining assay. (b, c) Quantitative data of the (b) live and (c) dead cells summarized from the live/dead cell staining assay. (d) Phalloidin staining showing the fibrous actin of the cytoskeleton of the cells. (e) Cell cytotoxicity of the hydrogels examined with CCK-8 assay. The hydrogels are biocompatible with the chondrocytes. NS: no significance.

Phalloidin staining was used to observe the fibrous actin of the cytoskeleton for the chondrocytes, and the results are shown in Fig. 4(d). The morphology of the cells in the three groups is complete and normal, which indicates that the hydrogels have good biocompatibility. The tetrazolium salt of CCK-8 is cleaved to a soluble formazan using live cells, and thus the absorbance is directly related to the number of viable cells. As displayed in Fig. 4(e), the CCK-8 test indicates that there are no significant differences between the experimental groups (GelMA and GelMA–PAM–PMPC) and the blank group at each time interval, and the number of viable cells is greatly increased on days 3 and 5 for GelMA and GelMA–PAM–PMPC. This further indicates that cell proliferation is not affected by co-culturing the chondrocytes with the hydrogels. In summary, the live/dead assay, phalloidin staining, and CCK-8 test all indicate that the hydrogels are biocompatible and have no cytotoxicity to chondrocytes.

Multiple factors are involved in the pathogenesis of osteoarthritis, such as reactive oxygen species, mechanical loading, and inflammatory cytokines (e.g., TNF-α and IL-1β). It is considered that chondrocyte degeneration, which is accepted to be the most significant feature of osteoarthritis, is closely related to the inflammatory cytokines. For example, inflammatory cytokines play an important role in the development of osteoarthritis, and the inflammatory environment contributes to extracellular matrix degradation and chondrocyte hypertrophy. The manifestation of osteoarthritis at the cellular level is due to the increase in catabolic genes and the degradation of anabolic genes. In this study, IL-1β and TNF-α were used to treat chondrocytes to mimic the symptoms of osteoarthritis. The protective effect of the drug-loaded hydrogels on chondrocyte degeneration was examined after co-culturing for 24 h. The mRNA expression levels of anabolic genes (aggrecan and COL2A1) and catabolic genes (MMP13 and ADAMTS5) were examined by RT-qPCR analysis. As displayed in Fig. 5, the mRNA expression of aggrecan and COL2A1 in the hydrogel samples (GelMA and GelMA–PAM–PMPC) is significantly higher than that of the blank group, and the mRNA expression of MMP13 and ADAMTS5 in the hydrogel samples is significantly lower than that of the blank group. These results indicate that the DS-loaded hydrogels have chondroprotective potential for inflammatory cytokine-induced chondrocytes, and consequently can be an effective scaffold for cartilage defects in the treatment of osteoarthritis.

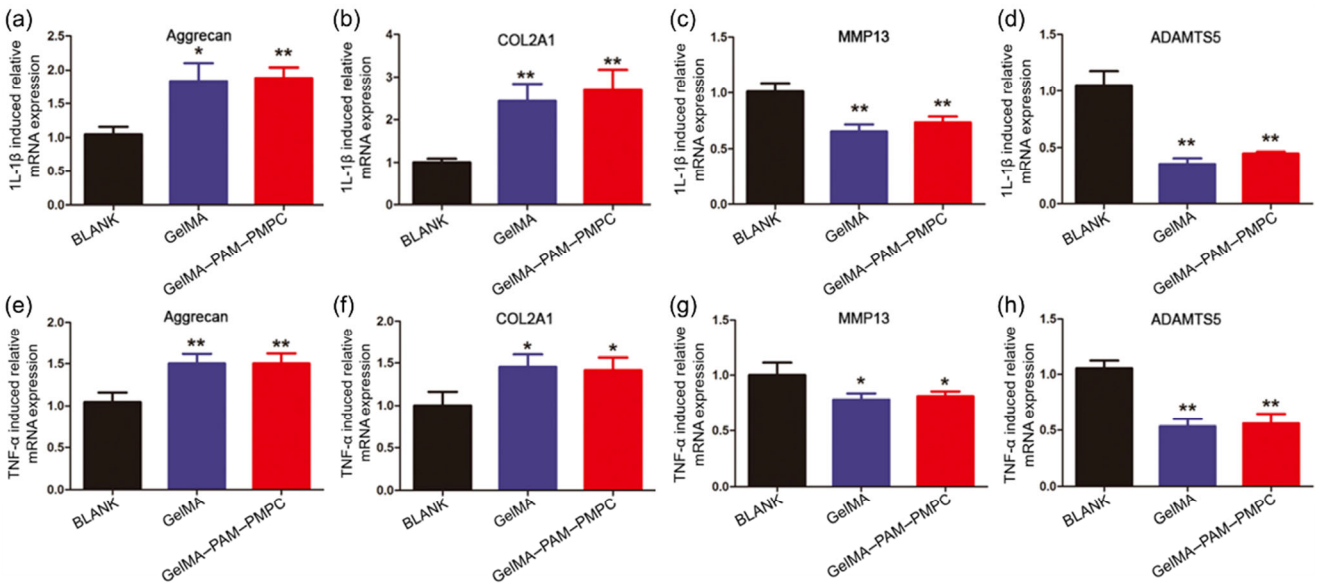

Fig. 5 RT-qPCR analysis showing the mRNA expression levels of anabolic genes (a, e) Aggrecan, (b, f) COL2A1, and catabolic genes (c, g) MMP13, (d, h) ADAMTS5 in IL-1β and TNF-α treated chondrocytes, which are incubated with the GelMA and GelMA–PAM–PMPC hydrogels. $n = 3$, $^{*}P < 0.05$, $^{**}P < 0.01$, compared with the blank group.

4 Conclusions

In this study, we successfully synthesized gelatin-based composite hydrogels, namely GelMA–PAM–PMPC, with biomimetic hydration lubrication and sustained drug release via photopolymerization, which could be used as a scaffold for cartilage defects in the treatment of osteoarthritis. The lubrication test indicated that the composite hydrogels maintained a relatively low COF under different experimental conditions and extended duration, which was attributed to the hydration lubrication mechanism of the zwitterionic phosphocholine headgroups. The drug release test showed that the composite hydrogels efficiently encapsulated the anti-inflammatory drug of DS and achieved a sustained release behavior. Additionally, the *in vitro* test demonstrated that the composite hydrogels were biocompatible and protected the chondrocytes from inflammatory cytokine-induced degeneration, upregulating the mRNA expression levels of anabolic genes and downregulating that of catabolic genes. In summary, the composite hydrogels prepared herein, with the dual functions of biomimetic hydration lubrication and sustained drug release, provide a promising approach for repairing cartilage defects in the treatment of osteoarthritis.

Acknowledgements

This study was financially supported by the National Natural Science Foundation of China (Nos. 51675296, 21868011, and 81772372), Shanghai Municipal Science Foundation (No. SYXF011803), Tsinghua University-Peking Union Medical College Hospital Initiative Scientific Research Program (No. 20191080593), the National Key R&D Program of China (No. 2017YFC1103800), Foshan-Tsinghua Innovation Special Fund (FTISF), Research Fund of State Key Laboratory of Tribology, Tsinghua University, China (No. SKLT-2020C11), and Ng Teng Fong Charitable Foundation (No. 202-276-132-13).

Electronic Supplementary Material: Supplementary material (synthesis of photopolymerization initiator, fabrication of polydimethylsiloxane ball, and calibration curve of diclofenac sodium) is available in the online version of this article at https://doi.org/10.1007/s40544-020-0437-5.

References

[1] Ji X, Yan Y, Sun T, Zhang Q, Wang Y, Zhang M, Zhang H, Zhao X. Glucosamine sulphate-loaded distearoyl phosphocholine liposomes for osteoarthritis treatment: combination of sustained drug release and improved lubrication. *Biomater Sci* **7**: 2716–2728 (2019)

[2] Zheng Y, Yang J, Liang J, Xu X, Cui W, Deng L, Zhang H. Bioinspired hyaluronic acid/phosphorylcholine polymer with enhanced lubrication and anti-inflammation. *Biomacromolecules* **20**: 4135–4142 (2019)

[3] Wan L, Wang Y, Tang X, Sun Y, Luo J, Zhang H. Biodegradable lubricating mesoporous silica nanoparticles for osteoarthritis therapy. *Friction* **10**(1): 68–79 (2022)

[4] Tan X, Sun Y, Sun T, Zhang H. Mechanised lubricating silica nanoparticles for on-command cargo release on simulated surfaces of joint cavities. *Chem Commun* **55**: 2593–2596 (2019)

[5] Pan Y, Xiao C, Tan H, Yuan G, Li J, Li S, Jia Y, Xiong D, Hu X, Niu X. Covalently injectable chitosan/chondroitin sulfate hydrogel integrated gelatin/heparin microspheres for soft tissue engineering. *Int J Polym Mater* **70**: 149–157 (2021)

[6] Wang M, Chen J, Li W, Zang F, Liu X, Qin S. Paclitaxel-nanoparticles-loaded double network hydrogel for local treatment of breast cancer after surgical resection. *Mater Sci Eng C Mater Biol Appl* **114**: 111046 (2020)

[7] Liu Y, Xiong D. Self-healable polyacrylic acid-polyacrylamide-ferric ion dual-crosslinked hydrogel with good biotribological performance as a load-bearing surface. *J Appl Polym Sci* **137**: 48499 (2019)

[8] Chen K, Chen G, Wei S, Yang X, Zhang D, Xu L. Preparation and property of high strength and low friction PVA-HA/PAA composite hydrogel using annealing treatment. *Mater Sci Eng C Mater Biol Appl* **91**: 579–588 (2018)

[9] Gong J, Katsuyama Y, Kurokawa T, Osada Y. Double-network hydrogels with extremely high mechanical strength. *Adv Mater* **15**: 1155–1158 (2003)

[10] Han L, Liu K, Wang M, Wang K, Fang L, Chen H, Zhou J, Lu X. Mussel-inspired adhesive and conductive hydrogel with long-lasting moisture and extreme temperature tolerance. *Adv Funct Mater* **28**: 1704195 (2018)

[11] Gan D, Xu T, Xing W, Ge X, Fang L, Wang K, Ren F, Lu X. Mussel-inspired contact-active antibacterial hydrogel with high cell affinity, toughness, and recoverability. *Adv Funct Mater* **29**: 1805964 (2019)

[12] Liu K, Han L, Tang P, Yang K, Gan D, Wang X, Wang K, Ren F, Fang L, Xu X, et al. An anisotropic hydrogel based on mussel-inspired conductive ferrofluid composed of electromagnetic nanohybrids. *Nano Lett* **19**: 8343–8356 (2019)

[13] Wang J, Lin L, Cheng Q, Jiang L. A strong bio-inspired layered pnipam-clay nanocomposite hydrogel. *Angew Chem Int Ed* **51**: 4676–4680 (2012)

[14] Dai X, Zhang Y, Gao L, Bai T, Wang W, Cui Y, Liu W. A mechanically strong, highly stable, thermoplastic, and self-healable supramolecular polymer hydrogel. *Adv Mater* **27**: 3566–3571 (2015)

[15] Wang H, Zhou L, Liao J, Ning C, Tan G. Cell-laden photocrosslinked gelma-dexma copolymer hydrogels with tunable mechanical properties for tissue engineering. *J Mater Sci Mater Med* **25**: 2173–2183 (2014)

[16] Visser J, Gawlitta D, Benders K E, Malda J. Endochondral bone formation in gelatin methacrylamide hydrogel with embedded cartilage-derived matrix particles. *Biomaterials* **37**: 174–182 (2015)

[17] Yue K, Santiago G T, Alvarez M M, Tamayol A, Annabi N, Khademhosseini A. Synthesis, properties, and biomedical applications of gelatin methacryloyl (gelma) hydrogels. *Biomaterials* **73**: 254–271 (2015)

[18] Elomaa L, Keshi E, Sauer I M, Weinhart M. Development of GelMA/PCL and dECM/PCL resins for 3D printing of acellular in vitro tissue scaffolds by stereolithography. *Mater Sci Eng C Mater Biol Appl* **112**: 110958 (2020)

[19] Su R, Zihlmann C, Akbari M, Tang X, Khademhosseini A. Reduced graphene oxide-gelma hybrid hydrogels as scaffolds for cardiac tissue engineering. *Small* **12**: 3677–3689 (2016)

[20] Yuk H, Zhang T, Lin S, Parada G A, Zhao X. Tough bonding of hydrogels to diverse non-porous surfaces. *Nat Mater* **15**: 190–196 (2016)

[21] Hu X, Vatankhah-Varnoosfaderani M, Zhou J, Li Q, Sheiko S S. Weak hydrogen bonding enables hard, strong, tough, and elastic hydrogels. *Adv Mater* **27**: 6899–6905 (2016)

[22] Jahn S, Seror J, Klein J. Lubrication of articular cartilage. *Annu Rev Biomed Eng* **18**: 235–258 (2016)

[23] Seror J, Merkher Y, Kampf N, Collinson L, Day A J, Maroudas A, Klein J. Normal and shear interactions between hyaluronan-aggrecan complexes mimicking possible boundary lubricants in articular cartilage in synovial joints. *Biomacromolecules* **13**: 3823–3832 (2012)

[24] Wang Y, Sun Y, Gu Y, Zhang H. Articular cartilage-inspired surface functionalization for enhanced lubrication. *Adv Mater Interfaces* **6**: 1900180 (2019)

[25] Klein J. Hydration lubrication. *Friction* **1**: 1–23 (2013)

[26] Moro T, Takatori Y, Ishihara K, Konno T, Takigawa Y, Matsushita T, Chung U, Nakamura K, Kawaguchi H. Surface grafting of artificial joints with a biocompatible polymer for preventing periprosthetic osteolysis. *Nat Mater* **3**: 829–836 (2004)

[27] Kyomoto M, Moro T, Saiga K, Miyaji F, Kawaguchi H, Takatori Y, Nakamura K, Ishihara K. Lubricity and stability of poly(2-methacryloyloxyethyl phosphorylcholine) polymer layer on Co–Cr–Mo surface for hemi-arthroplasty to prevent degeneration of articular cartilage. *Biomaterials* **31**: 658–668 (2010)

[28] Kyomoto M, Moro T, Yamane S, Hashimoto M, Takatori Y, Ishihara K. Poly(ether-ether-ketone) orthopedic bearing surface modified byself-initiated surface grafting of poly(2-methacryloyloxyethyl phosphorylcholine). *Biomaterials* **34**: 7829–7839 (2013)

[29] Daniele M A, Adams A A, Naciri J, North S H, Ligler F S. Interpenetrating networks based on gelatin methacrylamide and PEG formed using concurrent thiol click chemistries for hydrogel tissue engineering scaffolds. *Biomaterials* **35**: 1845–1856 (2014)

[30] Liu B, Wang Y, Miao Y, Zhang X, Fan Z, Singh G, Zhang X, Xu K, Li B, Hu Z, et al. Hydrogen bonds autonomously powered gelatin methacrylate hydrogels with super-elasticity, self-heal and underwater self-adhesion for sutureless skin and stomach surgery and E-skin. *Biomaterials* **171**: 83–96 (2018)

[31] Brown L, Zhang H, Blunt L, Barrans S. Reproduction of fretting wear at the stem-cement interface in total hip replacement. *Proc Inst Mech Eng Part H-J Eng Med* **221**: 963–971 (2007)

[32] Zhang H, Zhang S, Luo J, Liu Y, Qian S, Liang F, Huang Y. Investigation of protein adsorption mechanism and biotribological properties at simulated stem-cement

interface. *J Tribol-Trans ASME* **135**: 032301 (2013)
[33] Livak K J, Schmittgen T D. Analysis of relative gene expression data using real-time quantitative PCR and the 2(-Delta Delta C(T)) method. *Methods* **25**: 402–408 (2001)
[34] Yan Y, Sun T, Zhang H, Ji X, Sun Y, Zhao X, Deng L, Jin Q, Cui W, Santos H, et al. Euryale ferox seed-inspired superlubricated nanoparticles for treatment of osteoarthritis. *Adv Funct Mater* **29**: 1807559 (2019)
[35] Lin P, Zhang R, Wang X, Zhou F. Articular cartilage inspired bilayer tough hydrogel prepared by interfacial modulated polymerization showing excellent combination of high load-bearing and low friction performance. *ACS Macro Lett* **5**: 1191–1195 (2016)
[36] Shoaib T, Heintz J, Lopez-Berganza J A, Muro-Barrios R, Egner S A, Espinosa-Marzal R. Stick-slip friction reveals hydrogel lubrication mechanisms. *Langmuir* **34**: 756–765 (2018)
[37] Gombert Y, Simic R, Roncoroni F, Dubner M, Geue T, Spencer N D. Structuring hydrogel surfaces for tribology. *Adv Mater Interfaces* **6**: 1901320 (2019)
[38] Zhang X, Wang J, Jin H, Wang S, Song W. Bioinspired supramolecular lubricating hydrogel induced by shear force. *J Am Chem Soc* **140**: 3186–3189 (2018)
[39] Liu G, Cai M, Zhou F, Liu W. Charged polymer brushes-grafted hollow silica nanoparticles as a novel promising material for simultaneous joint lubrication and treatment. *J Phys Chem B* **118**: 4920–4931 (2014)
[40] Chen H, Sun T, Yan Y, Ji X, Sun Y, Zhao X, Qi J, Cui W, Deng L, Zhang H. Cartilage matrix-inspired biomimetic superlubricated nanospheres for treatment of osteoarthritis. *Biomaterials* **242**: 119931 (2020)
[41] Seror J, Zhu L, Goldberg R, Day A J, Klein J. Supramolecular synergy in the boundary lubrication of synovial joints. *Nat Commun* **6**: 6497 (2015)
[42] Ma S, Scaraggi M, Wang D, Zhou F. Stick-slip friction reveals hydrogel lubrication mechanisms. *Adv Func Mater* **25**: 7366–7374 (2016)

Kuan ZHANG. He received his B.S. in chemical engineering and technology in 2016 from Hainan University. He is currently a joint master student in Tsinghua University. His research interests include biotribology and soft materials.

Jielai YANG. He is a Ph.D. student at Department of Orthopedics & Shanghai Institute of Traumatology and Orthopedics, Ruijin Hospital, Shanghai Jiaotong University School of Medicine. His research focuses on the novel biomaterials for osteochondral regeneration and osteoarthritis management.

Hongyu ZHANG. He received his B.S. degree from Tianjin University, China (2005) and Ph.D. degree from University of Huddersfield, UK (2009). He is an associate professor at the State Key Laboratory of Tribology, Department of Mechanical Engineering, Tsinghua University, China. His research interests focus on the development of lubricating biomaterials such as nanoparticles, coatings, hydrogels, and electrospun nanofibers, which integrate the multi-disciplinary knowledge including biotribology, chemistry, materials science, and medicine to address clinical issues, e.g., osteoarthritis, anti-tissue/cell/bacteria adhesion, bone tissue engineering, etc.

Xiangyang XU. He is director of foot and ankle surgery, Ruijin Hospital, Shanghai Jiao Tong University School of Medicine. He is deputy director of foot and ankle surgery, Chinese Medical Association. He got his Ph.D. degree from Shanghai Medical University. His research focuses on diagnosis and treatment of diseases of the foot and ankle, with expertise in ankle instability and ankle osteoarthritis.

Bo WANG. He is a professor at College of Chemical and Biological Engineering, Shandong University of Science and Technology, China. He received his B.S. degree in Hainan University and Ph.D. degree in Zhejiang University, China. His research covers green chemistry, bio-catalysis, and asymmetric synthesis.